



Spatiotemporal trend analysis of precipitation, temperature, and soil moisture in selected agrarian locations within Nigeria—a comparative study

Blessing Funmbi Sasanya¹ · Akeem Abiodun Ademola² · Sunday Olufemi Adesogan²

Received: 12 March 2023 / Accepted: 18 June 2024 / Published online: 9 July 2024
© Saudi Society for Geosciences and Springer Nature Switzerland AG 2024

Abstract

Changes in trends and variabilities of precipitation, temperature, and evaporation are some of the pronounced effects of climate change. This study assessed the effects of precipitation and temperature trends and variabilities on soil moisture storage. Forty-one years' historical data on precipitation, temperature, and soil moisture were collected for four agrarian local government areas in southern and northern Nigeria. Trend changes and variabilities were analyzed using the Mann Kendall, modified Mann Kendall, Palmer drought severity index, standardized precipitation evaporation index, standardized precipitation index, and temperature indices. Observed precipitation in the northern part experienced very significant decrease and both the southern and northern divides experienced significant temperature increase over the last four decades. However, the temperature indices including hottest days (TXx), summer day (SU35), and diurnal temperature range (DTR) indicated northern Nigeria experienced more extreme temperature increase and thus more drought than southern Nigeria. The northern part had averages TXx, SU35, and DTR of 39.66 °C, 66.49 days, and 17.99 °C, while the southern part had 33.61 °C, 0.075 days, and 9.47 °C, respectively. The continuous increase in temperature and precipitation decrease are attributable to climate change caused by ozone layer depletion. Low precipitation and high temperature resulted to significant reduction of soil moisture storage in northern Nigeria, while soil moisture reductions were limited in southern Nigeria. Effects of temperature and precipitation trends on soil moisture trends therefore emphasize the need for proper water management, continuous soil moisture conservation, and intense irrigation practices, to enhance food production and security.

Keywords Trend analysis · Climate variability · Temperature indices · Precipitation indices · Soil moisture

Introduction

Global warming has prompted huge climatic variability all over the world (Zakwan and Ara 2019). Lately, several regions of the world are experiencing increased frequency and intensity of weather and climate extremes such as heat waves, wild fires, drought, storms, and flood. The percentage of cold nights is declining while that of warm nights keeps

increasing (Vincent et al. 2005). The impacts of climatic variability such as flooding, land slide, or drought have been felt by many developing countries and such nations are left in a terrible state after the impacts. The issue of climate change, fluctuations, variations, and trend is therefore no longer arguable. The controversial issue is the nature of this change, fluctuations, variations, and trend in specific regions especially in arid and semi-arid regions such as northern Nigeria.

The important influences of the climatic variability are precipitation and temperature (Bhuyan et al. 2018). The primary source of fresh water on earth is precipitation (Anil and Ramesh 2017). Changes in properties of precipitation, such as its amount, spatial and temporal variabilities, type, and trends are expected, resulting from increased evaporation to the atmosphere preceded by global warming. These properties of precipitation are some of the most important factors affecting agricultural production (Khavse et al.

Responsible Editor: Zhihua Zhang

✉ Blessing Funmbi Sasanya
blessing.env@gmail.com

¹ Department of Crop and Soil Science, Faculty of Agriculture, University of Port Harcourt, Port Harcourt, Nigeria

² Department of Civil Engineering, Faculty of Technology, University of Ibadan, Ibadan, Nigeria

2015). Soil moisture is also a determining factor in numerous complex environmental processes and their amount is influenced by precipitation (Patel et al. 2008). The variation and distribution of soil moisture in space and time are unique factors that are commensurate to energy exchange in the ecosystems of vegetation, soil, and atmosphere (Patel et al. 2008). The variation of soil moisture as a factor aids the evaluation of energy exchanged between the vegetation, soil, and atmosphere, thus as it serves as control for hydrological, meteorological, and agricultural processes (Tao et al. 2021). Thorough assessment and monitoring of soil moisture are thus of critical importance in arid and semi-arid regions, where deficit of water is becoming a limiting factor restricting ecological development and agricultural productivity.

Climate change often influences irregular precipitation pattern and increasing extreme temperature indices, most especially in arid and semi-arid regions such as were experienced in some African countries, including Ethiopia, Tanzania, and Kenya (Gebrechorkos et al. 2019). The increasing temperature and reduction in precipitation amount will lead to rise in atmospheric evaporative demand which will thus result to gross depletion in cumulative soil moisture (Wang et al. 2016). Drought (insufficient precipitation in geographical location over a long period of time) can also lead to deficit in soil moisture content. Drought is a complex environmental phenomenon which can create severe impact on socioeconomic activities, personal life, and agricultural sector (Wang et al. 2016). Droughts are monitored by various elements and their interactions, including soil and vegetation information, meteorological forces, and variability and human factors including agricultural management practices choices such as grazing density and irrigation systems (Van Loon et al. 2016).

Series of research have employed trends and indices to investigate the temporal and spatial variability of temperature and precipitation in various geographical locations. For instance, Salameh et al. (2022) studied the spatial and temporal variability of extreme rainfall in Southern Levant and related large-scale atmospheric circulation pattern. Increasing period of extreme dry spell during spring was reported for the study area. Adakayi et al. (2016) also assessed the pattern of rainfall in Northern Nigeria and also predicted a significant increase in trend of precipitation between 2020 and 2030. The Mann Kendall trend test was employed by Asfaw et al. (2018) to detect the trend changes in precipitation and the result indicated intra-annual and inter-annual variabilities with increase in the trend and period of drought years. Goswami et al. (2006) also analyzed precipitation data of different countries in Asia and revealed that annual precipitation decreased in India. Yadav et al. (2014), in another study, revealed that trends of precipitation and temperature are increased in some months and reduced in some others based on analyses carried out in some 13 different districts

of Uttarakhand, India. Furthermore, Alhaji et al. (2018) claimed positive value for Kendall's statistics (Z) for average and maximum temperature in Gombe State, Nigeria. Similarly, Pal et al. (2017) suggested the presence of warming trends in the Dadeldhura district of Nepal. Salameh et al. (2019) analyzed the spatio-temporal extreme temperature over the Levant region. It was discovered from the study that highest values of annual minimum temperature increased with about 0.68 °C per decade.

Furthermore, Oufrigh et al. (2023) analyzed monthly and seasonal rainfall around the Coastal Oran and Macta watershed in North West of Algeria using the Mann Kendall and the innovative trend analysis (ITA) method. The ITA method applied detected that 63% of the station shows increasing trend and 31% decreasing trends in seasonal rainfall. Aamir et al. (2022) found monotonic trends in monthly rainfall of Baluhistan from the MK tests. Sneha and Uma (2023) also used the MK and Theil's slope approach to analyze the annual and seasonal rainfall trends India. Declines were detected during the winter while there were increases in the pre-monsoon, monsoon, and post-monsoon seasons. Decline in rainfall was also reported on the annual basis.

In the same vein, several other drought indices and methods for soil moisture retrieval have been proposed in previous series of research. Szép et al. (2005) employed the Palmer drought severity index (PDSI) to analyze the homogenized 99-year (1901–1999) monthly precipitation and temperature data series at three stations in West-Hungary. Conditions of local soil moisture were revealed to be drier, as parallel to the changes in hemisphere in the twentieth century. Bong and Richard (2020) assessed drought and climate change in Sarawak River basin, Malaysia, by fitting 41-year (1975–2016) monthly precipitation data from 15 rainfall stations to standardized precipitation indices (SPI). A declining trend values indicated a higher tendency of increased drought event in the basin. Adesogan and Sasanya (2021) also used SPI, rainfall anomaly index (RAI), and rainfall decile index (RDI) to assess water availability in a part of south-western Nigeria. Tam et al. (2019) projected drought in Canada using the standardized precipitation and evaporative index (SPEI). An increase in wetting during winter and spring and increase in drying during autumn and summer were projected. Eze (2018) also employed the normalized rainfall index (NRI) to determine the droughts extent and its implications on households in Yobe state, Nigeria. Ali et al. (2010) proposed the normalized antecedent precipitation index (NAPI), and applied it to three watersheds, to simulate runoff yield in the semi-arid region of India. Ndlovu and Demlie (2020) employed percent of normal precipitation index (PNPI) and RAI to explore and categorize the wet and dry periods in 18 selected rainfall gauging stations across the KwaZulu-Natal province of South Africa. SPI and PNPI were employed by Mahajan and Dodamani (2016)

to study the temporal and spatial variation of drought incidences observed from 52-year (1960–2012) monthly precipitation data recorded by 59 rain gauge stations in Krishna basin, Maharashtra. Zeri et al. (2018) used soil moisture index based on a normalization of soil moisture by wilting point and field capacity to characterize the exact soil moisture conditions into severe drought category to very wet category in Brazil.

Having assessed the existing body of knowledge, none of the studies have assessed the relationship and similarities or otherwise in the trends and variability of precipitation, temperature, and soil moisture (at different depths) especially in areas with heavy agricultural activities in recent times. This study hypothesized that the trends and variability of rainfall and temperature have pronounced effects on the trend and variability of soil moisture in a particular region. The aim of this study is therefore to investigate the relationships and similarities or otherwise in the trend changes and variability of precipitation, temperature, and soil moisture (at different depths) in two local government areas of Katsina state (Northern Nigeria) and two local government area of Rivers state (Southern Nigeria), Nigeria, where agricultural practices are prominent using 41 years' historical observations. These were achieved by the use of the Mann-Kendall tests (for trend time series analysis of precipitation, temperature, and soil moisture), drought indices (for precipitation and soil moisture), and temperature indices (for minimum and maximum) temperature. Soil moisture studies are of extreme importance, because soil moisture decline always precedes decreased soil respiration, decreased biomass production, and also decrease in overall soil carbon balance which leads to food insecurity (Vargas et al. 2018). It is therefore crucial to determine and compare the trends and indices indicating the variability of precipitation, temperature, and soil moisture on agricultural sites in southern (tropical region) and northern (semi-arid region) Nigeria, where water deficit is gradually becoming a hindrance to the development of agricultural and ecological activities.

Materials and methods

Study area and data collection

Forty-one-year (1981–2021) daily and monthly data on precipitation, minimum temperature, maximum temperature, soil moisture (0–5cm depth), and soil moisture

(0–100 cm depth) were obtained for four different areas in southern and northern Nigeria. These data were obtained from the official website of the National Aeronautic Space and Administration (NASA) (<https://power.larc.nasa.gov/data-access-viewer/>). The data is defined by a worldwide grid with a spatial resolution of $0.1^\circ \times 0.1^\circ$ in latitude and longitude, equivalent to a grid size of around 10 km (Sasanya et al. 2024). Geographical coordinates for each data point within each local government area (LGAs) were determined using their respective administrative headquarters. Studies including Espinoza-Dávalos et al. (2015), Sharma et al. (2020), and Sasanya et al. (2024) had used data from the same source.

Figure 1 delineates the four local government areas studied in northern and southern Nigeria. Danja (longitude 7.554°E , latitude 11.384°N) and Faskari (longitude 7.027°E , latitude 11.727°N) are local governments in the northern area, while Obio/Akpor (longitude 7.0284°E , latitude 4.861°N) and Tai (longitude 7.242°E , latitude 4.767°N) are of the southern Nigeria. From the collected data, Danja and Faskari experienced average annual precipitation of 1025.25 and 1009.17 mm, respectively, while Obio/Akpor and Tai receive average precipitation of 2618.07 and 2423.42 mm in the same order, annually. Driest periods in the northern parts studied span from November to March, while the rainy seasons are experienced from April to October annually (Ibebuchi and Abu 2023).

The southern parts received much longer periods of rainfall spanning from March to October. Even the dry seasons sometimes receive some millimeters of precipitation annually at intervals, although these are not always as much as those received during the rainy season (Ibebuchi and Abu 2023).

Evapotranspiration data

According to Adesogan and Sasanya (2023), evapotranspiration values estimated from FAO Penman Monteith equation are close to those measured from Pan and Piche evaporimeter. The FAO Penman Monteith equation was reported to perform better than Thorntwaite, Hargreves-Samani, Hamon, and the Blaney Criddle methods. Data on evapotranspiration for this study were therefore estimated from maximum and minimum temperatures, maximum and minimum relative humidities, and wind velocity (U_2) at 2 m height (m/s), using the Penman Monteith models given as Eq. (1).

$$PET = \frac{0.408\Delta(R_n - G) + \gamma \frac{900}{T+273} U_2 (e_s - e_a)}{\Delta + \gamma (1 + 0.34 U_2)} \quad (1)$$

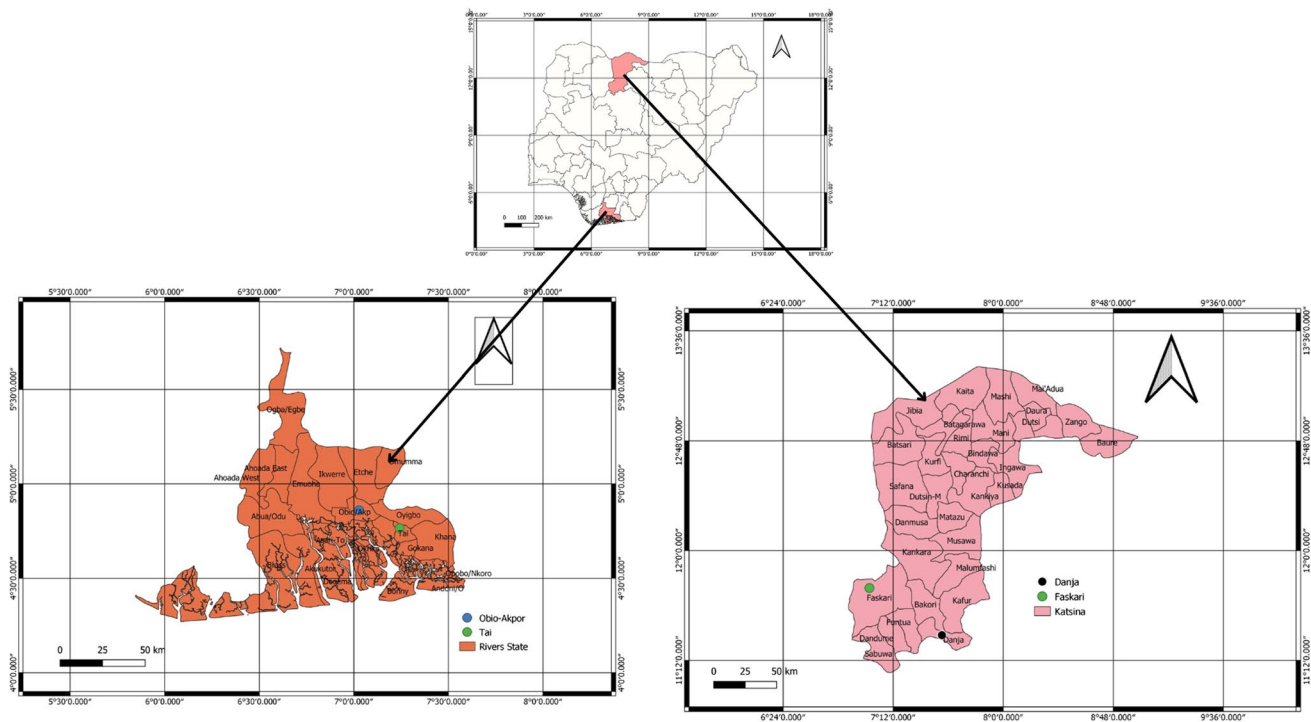


Fig. 1 Map of Katsina and Rivers States, Nigeria, delineating various local government and study areas

where R_n = average net radiation at the crop surface ($\text{MJ}/\text{m}^2/\text{day}$), G is soil flux density ($\text{MJ}/\text{m}^2/\text{day}$), γ = psychrometric constant ($\text{kPa}/^\circ\text{C}$) = 0.067, e_s = saturation vapor pressure (kPa), e_a = actual vapor pressure (kPa), $e_s - e_a$ = saturation vapor pressure deficit (kPa), T = air temperature at 2 m height ($^\circ\text{C}$), Δ = slope vapor pressure curve ($\text{kPa}/^\circ\text{C}$).

Mann Kendall tests

The Mann-Kendall (MK) (non-parametric) test is utilized to recognize an ascending or descending trend (monotonic patterns) in a progression of hydrological information and environmental data. The test is widely used for environmental applications, because of their simplicity, non-assumption of distribution residuals, and its ability to take care of outliers and missing values (Revadekar et al. 2012). The null hypothesis (H_0) shows no trend while the alternative hypothesis (H_1) shows a trend in a one-sided or two-sided test as an upward trend or downward trend (Paul et al. 2023). This is used for observing statistically significant trends in variables like rainfall, temperature, stream flow, and soil moisture.

In this study, the Mann Kendall test is used to analyze the trend of the data detected. The Mann Kendall statistic (S) for trend is given as

$$S = \sum_{l=1}^{n-1} \left(\sum_{j=l+1}^n \text{sgn} (R_i - R_j) \right) \quad (2)$$

where n is the data set length, and R_i and R_j are the subsequent data values.

$$\text{Sgn}(x) = \begin{cases} 1 & \text{if } x > 0 \\ 0 & \text{if } x = 0 \\ -1 & \text{if } x < 0 \end{cases} \quad (3)$$

It has been documented that when n is greater than 8 or if hypothesis (H_0) is true, the test statistics (S) is approximately normally distributed (Schweinsberg et al. 2021) with mean and variance given as Eqs. (4) and (5). The Mann Kendall Z statistics is thus computed from Eq. (6).

$$E(S) = 0 \quad (4)$$

$$\text{Var}(S) = n \frac{(n-1)(2n+5)}{18} \quad (5)$$

$$Z = \begin{cases} \frac{S-1}{\text{Var}(S)} & \\ 0 & \\ \frac{S+1}{\text{Var}(S)} & \end{cases} \quad (6)$$

If the MK Z statistic follows normal distribution, a positive Z indicates an increasing trend and negative Z indicates a downward trend for the period (Nath et al. 2024). When a significant α -level is reached, $Z \geq Z_{\alpha/2}$, the data trend is

considered significant. The formula above is well grounded if the number of observation (n) exceeds 10 (Nath et al. 2024). This test was done for each month, using the “mk.test” function in R programming language.

Modified Mann-Kendall tests

The modified Mann-Kendall detected the trends of temperature, rainfall, and soil moisture of data with significant autocorrelation coefficients. For this study, the modified Mann Kendall test was only conducted on months whose autocorrelation coefficients exceeded positive or negative 0.31 as detected from the autocorrelation (ACF) and partial autocorrelation test (PACF). The bias corrected pre-whitening (“bcpw”) package on R Studio was used to perform the modified Mann-Kendall test (O’Brien et al. 2021) on all datasets. In accordance to the Mann Kendall’s test, positive non-parametric correlation coefficient (τ) or Sen’s slope shows concordance or increasing trends, while a negative τ or Sen’s slope values show discordance or decreasing trends. The Sen’s slope enabled the determination of magnitude of the detected trend (Mathivha and Mbatha 2022).

Palmer drought severity index (PDSI)

The Palmer drought severity index (PDSI) measures the spatial and temporal departure of cumulative moisture supply (Palmer 1965). The PDSI makes use of the Thornthwaite method to derive potential evapotranspiration. The PDSI calculation is based on a simple two-layer soil model based on water supply and demand rather than variation in rainfall. The simple two-layer model is also based on four assumptions, which are (i) moisture has to be removed from the surface layer first before it is being removed from the lower soil layer; (ii) runoff can only occur when the surface and lower soil layers are both fully saturated; (iii) evapotranspiration loss occurs at a potential rate from the surface layer; (iv) evapotranspiration loss depends on the initial moisture content of the lower soil layer and the combined available water holding capacity (AWC) of the two layers of the soil (Alley 1984). The variables needed for the estimation of PDSI are evapotranspiration (ET), runoff (RO), recharge (R), potential evapotranspiration (PET), potential recharge (PR), loss (L), potential loss (PL), and the amount of water exchanged between the two soil layers, that is, precipitation (p) as given by the Eq. (7).

$$p = \alpha PET + \beta PR + \gamma PRO - \delta PL \quad (7)$$

where p is the amount of precipitation needed to maintain a normal soil moisture level for a given month; PET is potential evapotranspiration; PR represents potential soil water recharge; PRO represents potential runoff; and PL represents

loss and α , β , γ , and δ are their respective coefficients (called the weighing factors). These coefficients are estimated from Eq. (8).

$$\alpha = \frac{ET}{PET}; \beta = \frac{R}{PR}; \gamma = \frac{RO}{PRO}; \delta = \frac{L}{PL} \quad (8)$$

Moisture departure (d) is the difference between the actual precipitation (P) in a month under consideration and the estimated precipitation (p) under the existing conditions. The term d can be estimated from Eq. (9).

$$d = P - p = P - (\alpha PE + \beta PR + \gamma PRO - \delta PL) \quad (9)$$

The spatial and temporal meaning of the moisture departure can be different for surface water balance (Zhang et al. 2019). In order to have a good correlation, the moisture departure was weighted by a climate characteristic coefficient (K) estimated from Eq. (10).

$$K = \frac{17.67}{\sum_{j=1}^{12} d_j K_j} K_j \quad (10)$$

The multiplication of K and d gives the moisture anomaly index, Z . The Z index indicates the degree or wetness or dryness within a particular month, without considering the recent precipitation trends (Ogunrinde et al. 2020). The PDSI values (X_i) are obtainable from each Z index for a given month, using the relationship given in Eq. (11).

$$X_i = 0.897 X_{i-1} + \left(\frac{1}{3}\right) Z_i \quad (11)$$

where X_i represents the PDSI value of the current month, $X_{(i-1)}$ is the PDSI value of the previous month, and the values 0.897 and $1/3$ are the duration factors. Table 1 shows the PDSI wetness and dryness grading standards as extracted from Zhang et al. (2019). The PDSI values in this study were estimated using the “scpdsi” package on R studio.

Standardized precipitation evaporation index (SPEI)

The standard precipitation evaporation index (SPEI) is built on temperature and precipitation data (Wu et al. 2021). The advantage of SPEI is its ability to integrate numerous characters with the effects of temperature variability on drought assessment (Vicente-Serrano et al. 2010). Potential evapotranspiration (PET) and rainfall data are required in the computation of SPEI (Nury et al. 2017; Vicente-Serrano et al. 2018). The PET for this study was estimated from the Penman Montith’s model. The input data for the estimation of SPEI was the difference (D) between the precipitation (P) and PET for each month (Nury et al. 2017; Vicente-Serrano et al. 2018; Wu et al. 2021).

The estimated value of D_i was done in time step of 1-month interval for 41 years. The difference in a given month j and

Table 1 Palmer drought severity index (PDSI) dryness/wetness grades

| PDSI | Wet and dry grade | PDSI | Wet and dry grade |
|-------|-------------------|--------------|-------------------|
| ≥ 4 | Extremely wet | ≥ - 2 to - 1 | Mild drought |
| ≥ 3-4 | Very wet | ≥ - 3 to - 2 | Moderate drought |
| ≥ 2-3 | Moderately wet | ≥ - 4 to - 3 | Severe drought |
| ≥ 1-2 | Slightly wet | < - 4 | Extreme drought |

Source: Zhang et al. (2019)

year i depends on the time steps (k) selected, which is three in this case. According to Ogunrinde et al. (2020), the time step equations are given as Eqs. (12) and (13).

$$X_{ij}^k = \sum_{i=13-j-k}^{12} D_{i-1,l} + \sum_{i=1}^j D_{i,l} \text{ for } j \leq k \text{ and} \quad (12)$$

$$X_{ij}^k = \sum_{i=j-k+1}^j D_{i-1,l} \text{ for } j \geq k \quad (13)$$

The difference (D_i) was thereafter integrated to a three-parameter log-logistic distribution. The probability density function of the three factor log-logistic distribution is given as

$$f(x) = \frac{\beta}{\alpha} \left(\frac{x-\gamma}{\alpha} \right)^{\beta-1} \left(1 + \left(\frac{x-\gamma}{\alpha} \right)^{\beta} \right)^{-2} \quad (14)$$

where α represents scale parameter, β represents shape parameter, and γ represents origin parameter for values of D following the range ($\gamma > D > \infty$). The L-moment method (Ahmad et al. 1988) was used to determine the parameters of the log-logistic distribution. The cumulative density function was obtained from Eq. (14). The standardized form of $F(x)$ resulted in the SPEI values.

$$F(x) = \left(1 + \left(\frac{x-\gamma}{\alpha} \right)^{\beta} \right)^{-1} \quad (15)$$

The SPEI function on the R programming language was employed to determine the SPEI values for the study areas. SPEI values obtained for each monthly precipitation were classified as shown in Table 2.

Standardized precipitation index (SPI)

The standardized precipitation index (SPI) was used to determine the degree of wetness and dryness for precipitation values and also soil moisture values (depths 0–5 cm and 0–100 cm) for the study areas. The SPI is useful in assessing drought conditions over a long period of time. This was subjected to probability distribution using the gamma function for a long-term precipitation (McKee et al. 1993). This index has proved to give a reliable severity estimate value for spatial analysis of

Table 2 Class descriptions for SPI and SPEI

| SPI/SPEI | Class description | SPI/SPEI | Class description |
|----------|-------------------|-----------------|-------------------|
| > = 2 | Extremely wet | - 0.99 to 0.9 | Normal |
| 1.5-1.99 | Very wet | - 1 to - 1.49 | Moderately dry |
| 1-1.49 | Moderately wet | - 1.5 to - 1.99 | Very dry |
| | | < = - 2 | Extremely dry |

Source: Shen et al. (2003); Adesogan and Sasanya (2021)

droughts. Normalized numerical values are given to the long-term data and the deviation from the long-term mean of the precipitation under consideration for the random variables that are normally distributed is given as the SPI (Tirivarombo et al. 2018; Adesogan and Sasanya 2021). The SPI becomes positive when precipitation rises above the long-term mean and the SPI is negative otherwise. SPI values for each time step are obtained by fitting precipitation data to the cumulative density function (CDF) of gamma distribution (Al-timimi and Osamah 2016; Adesogan and Sasanya 2021), given as Eq. (16).

$$G(x) = \int_0^x \frac{1}{\beta^{\alpha}\Gamma(\alpha)} x^{\alpha-1} e^{-\left(\frac{x}{\beta}\right)} dx \quad (16)$$

$$\alpha = \frac{1}{4A} \left(1 + \sqrt{1 + \frac{4A}{3}} \right) \quad (17)$$

$$\beta = \frac{X_a}{\alpha} \quad (18)$$

$$A = \ln(X_a) - \frac{\ln\left(\sum(\bar{X})\right)}{n} \quad (19)$$

$$H(x) = q + (1 - q) G(x) \quad (20)$$

where n is the number of years, α and β are the respective scale and shape parameter of the CDF, X is the annual precipitation amount (mm), and \bar{X} is the average value of the annual precipitation (mm). The gamma distribution for a zero precipitation amount is not defined is are thus taken care of by Eq. (19), q is the probability of zero value which is given as m/n , where m = number of zero values and n = total number of observations. The SPEI values obtained for each monthly precipitation were classified as shown in Table 2.

Temperature indices

The extreme temperature indices such as annual means recommended by the Expert Team on Climate Change

Detection and Indices (ETCCDI) of the World Meteorological Organization (WMO) were used to analyze temperature trends and also detect change in the climate. These extreme temperature indices including absolute, percentile-based, threshold, and other indices essentially represent changes in frequency, intensity, and duration of minimum and maximum temperatures. These indices were computed to monitor the temperature trend for each local government area. The indices are shown on Table 3 as adapted from Revadekar et al. (2012), Yin and Sun (2018), and Limsakul (2020).

Results and discussions

Variabilities and trend analyses of precipitation and temperature

Results on the time series trend analysis of rainfall and temperature and their resultant effects on the trends of soil moisture (at 95% level of confidence), investigated in four agrarian local government areas in the northern (semi-arid) and southern (tropical) divides of Nigeria, using 41 years' recent historical observations (1981 to 2021) are presented on Tables 4, 5, 6, 7, and 8. Figures 2, 3, 4, 5, and 6 are pictorial representations of various drought indices used for the assessment of precipitation and soil moisture. The trends of monthly precipitation as rainfall in the humid southern part of Nigeria (Tai and Obi-Akpor) were majorly observed to be

negative or decreasing. However, in Tai, the month of May had significantly negative trend, while January, August, and November had increasing trends at 5% level of significance. Trends of monthly rainfall in Obio-Akpor are closely related to those of Tai. However, the negative trends of rainfall during October and April were significant. In contrast, monthly rainfall observations in the semi-arid regions experienced more significant downward trends than those in the south.

In the semi-arid regions, Januarys and Februarys were consistently dry with no drop of rainfall (Table 4). Trends of historical precipitation events in Danja were significantly negative during supposedly peak rainy seasons in the southern region, that is, in May, June, August, and September. The same trends were observed in Faskari. Trends of historical monthly rainfall were significantly negative in May, June, and September. Trends of total annual precipitation in the semi-arid regions were significantly negative, while only mildly decreasing trends were observed in the southern region.

These finding gave credence to the claims of Lema and Majule (2009) and Begizew (2021) stating that the semi-arid regions of Nigeria are characterized by low and fast-decreasing precipitation amounts. These characteristic low and decreasing precipitations are fast becoming more intense, due to climate change (Tabari 2020; Clarke et al. 2022). In accordance to the claims of Feng et al. (2013), the tropics experience more rainfall amount over the same period of time. Although, trends of rainfall were observed to be decreasing generally;

Table 3 Description of temperature indices and units employed in the study as described by WMO

| Indices | Descriptive name | Definition | Unit |
|------------------------------------|----------------------------------|--|------|
| Extremely warm temperature indices | | | |
| TN90p | Warm nights | Days with minimum temperature above 90th percentile (TN > 90th percentile) in a year (1982–2021) | % |
| TX90p | Warm days | Days with maximum temperature is above 90th percentile (TX > 90th percentile) in a year (1982–2021) | % |
| TNx | Temperature min. (hottest night) | Highest daily minimum temperature value in a year (1982–2021) | °C |
| TXx | Temperature max. (hottest day) | Hottest daily maximum temperature value in a year (1982–2021) | °C |
| TR25 | Tropical night | Number of days when minimum temperature TN is above 25 °C in a year (1982–2021) | Days |
| SU35 | Summer days | Number of days when maximum temperature TX is above 35 °C in a year (1982–2021) | Days |
| Extremely cold temperature indices | | | |
| TN10p | Cold nights | Days when minimum temperature below 10th percentile (TN < 10th percentile) in a year (1982–2021) | % |
| TX10p | Cold days | Days with maximum temperature below 10 th percentile (TX < 10th percentile) in a year (1982–2021) | % |
| TNn | Temperature min. (coldest night) | Lowest daily minimum temperature value in a year (1982–2021) | °C |
| TXn | Temperature max. (coldest day) | Lowest daily maximum temperature value in a year (1982–2021) | °C |
| TX15 | Cold days | Number of days when maximum temperature below 15 °C in a year (1982–2021) | Days |
| TX10 | Cold nights | Number of days when minimum temperature below 10 °C in a year (1982–2021) | Days |
| DTR | Diurnal temperature range | Mean difference between daily maximum and minimum temperatures in a year (1982–2021) | °C |

Source: Revadekar et al. (2012), Yin and Sun (2018), and Limsakul (2020)

Table 4 Trend analysis of rainfall in LGAs of southern and northern Nigeria

| Parameters | Jan. | Feb. | Mar. | Apr. | May | Jun. | Jul. | Aug. | Sept. | Oct. | Nov. | Dec. | Annual |
|-------------------------|--------|---------|--------|---------|---------|---------|---------|---------|---------|---------|-------|---------|---------|
| Southern Nigeria | | | | | | | | | | | | | |
| Tai | | | | | | | | | | | | | |
| τ | 0.030 | -0.066 | -0.040 | -0.193 | -0.219 | -0.053 | -0.027 | 0.028 | -0.012 | -0.169 | 0.096 | -0.038 | -0.071 |
| S | 22.00 | -53.00 | -32.00 | -157.00 | -178.00 | -43.00 | -22.00 | 23.00 | -10.00 | 138.00 | 78.00 | -28.00 | -58.00 |
| Z value | 0.246 | -0.586 | -0.349 | -1.754 | -1.991 | -0.472 | -0.236 | 0.247 | -0.101 | -1.539 | 0.866 | -0.318 | -0.640 |
| p value | 0.806 | 0.558 | 0.727 | 0.080 | 0.047 | 0.637 | 0.813 | 0.805 | 0.919 | 0.124 | 0.387 | 0.751 | 0.522 |
| ACF | -0.115 | -0.333 | -0.110 | 0.193 | 0.274 | 0.091 | 0.100 | 0.205 | 0.137 | 0.208 | 0.120 | -0.089 | 0.351 |
| Sen slope | na | -0.162 | na | na | na | na | na | na | na | na | na | na | -4.699 |
| Obio Akpor | | | | | | | | | | | | | |
| τ | -0.054 | -0.160 | -0.097 | -0.239 | -0.173 | -0.068 | -0.063 | -0.031 | -0.040 | -0.225 | 0.081 | -0.071 | -0.111 |
| S | -40.00 | -128.00 | -79.00 | -194.00 | -141.00 | -56.00 | -51.00 | -26.00 | -33.00 | -183.00 | 66.00 | -53.00 | -91.00 |
| Z value | -0.456 | -1.43 | -0.877 | -2.169 | -1.573 | -0.618 | -0.562 | -0.281 | -0.360 | -2.046 | 0.731 | -0.608 | -1.011 |
| p value | 0.648 | 0.152 | 0.380 | 0.030 | 0.116 | 0.537 | 0.574 | 0.778 | 0.719 | 0.041 | 0.465 | 0.543 | 0.312 |
| ACF | -0.054 | -0.023 | 0.050 | 0.221 | -0.205 | 0.142 | 0.135 | 0.227 | 0.120 | 0.225 | 0.265 | -0.040 | 0.438 |
| Sen slope | na | na | na | na | na | na | na | na | na | na | na | na | -12.013 |
| Northern Nigeria | | | | | | | | | | | | | |
| Danja | | | | | | | | | | | | | |
| τ | na | na | -0.068 | -0.198 | -0.226 | -2.442 | -0.076 | -0.260 | -2.353 | -0.114 | 0.131 | 0.221 | -0.210 |
| S | na | na | -31.00 | 156.00 | -183.00 | -218.00 | -62.00 | -210.00 | -210.00 | 92.00 | 56.00 | 40.00 | -172.00 |
| Z value | na | na | -0.518 | -1.756 | 2.407 | -2.105 | 0.6857 | -2.353 | -0.261 | -1.025 | 1.010 | 1.648 | -1.921 |
| p value | na | na | 0.604 | 0.079 | 0.041 | 0.035 | 0.493 | 0.019 | 0.019 | 0.305 | 0.312 | 0.099 | 0.054 |
| ACF | na | na | 0.059 | -0.085 | 0.238 | 0.128 | 0.223 | 0.209 | -0.040 | 0.073 | 0.306 | -0.0001 | 0.265 |
| Sen slope | na | na | na | na | na | na | na | v | na | na | na | na | na |
| Faskari | | | | | | | | | | | | | |
| τ | na | na | -0.102 | -0.211 | -0.292 | -0.263 | -0.190 | -0.086 | -0.247 | -0.009 | 0.206 | 0.221 | -0.242 |
| S | na | na | -36.00 | -166.00 | -236.00 | -213.00 | -154.00 | -70.00 | -200.00 | -7.00 | 73.00 | 40.00 | -198.00 |
| Z value | na | na | -0.768 | -2.644 | -2.644 | -2.384 | -1.720 | -0.776 | -2.239 | -0.068 | 1.579 | 1.648 | -2.213 |
| p value | na | na | 0.443 | 0.062 | 0.008 | 0.017 | 0.085 | 0.438 | 0.025 | 0.946 | 0.114 | 0.099 | 0.027 |
| ACF | na | na | -0.087 | -0.186 | 0.308 | 0.209 | 0.256 | 0.222 | -0.025 | -0.048 | 0.231 | -0.0006 | 0.336 |
| Sen slope | na | na | na | na | -1.582 | na | na | na | na | na | na | na | na |

τ is the Kendall rank correlation coefficient, S is the Kendall statistics, ACF is the autocorrelation coefficient, and Z and p values compare level of significance of Kendall statistics

Table 5 Trend analysis of average temperature in LGAs of southern and northern Nigeria

| Parameters | Jan. | Feb. | Mar. | Apr. | May | Jun. | Jul. | Aug. | Sept. | Oct. | Nov. | Dec. | Annual |
|------------------|---------|---------|--------|--------|--------|--------|--------|--------|--------|--------|--------|--------|--------|
| Southern Nigeria | | | | | | | | | | | | | |
| Tai | | | | | | | | | | | | | |
| τ | 0.234 | 0.318 | 0.346 | 0.407 | 0.565 | 0.533 | 0.631 | 0.549 | 0.561 | 0.563 | 0.535 | 0.496 | 0.639 |
| S | 192.00 | 260.00 | 282.00 | 332.00 | 462.00 | 435.00 | 515.00 | 448.00 | 459.00 | 459.00 | 438.00 | 324.00 | 521.00 |
| Z value | 2.146 | 2.910 | 3.158 | 3.720 | 5.179 | 4.877 | 5.776 | 5.02 | 5.146 | 5.148 | 4.910 | 3.629 | 5.844 |
| p value | 0.032 | 0.004 | 0.002 | 0.000 | 0.000 | 0.000 | 0.000 | 0.000 | 0.000 | 0.000 | 0.000 | 0.000 | 0.000 |
| ACF | - 0.015 | - 0.026 | 0.091 | 0.143 | 0.538 | 0.463 | 0.615 | 0.517 | 0.55 | 0.508 | 0.570 | 0.239 | 0.674 |
| Sen slope | na | na | na | na | 0.026 | 0.025 | 0.029 | 0.024 | 0.025 | 0.026 | 0.033 | na | 0.028 |
| Obio Akpor | | | | | | | | | | | | | |
| τ | 0.214 | 0.313 | 0.311 | 0.422 | 0.576 | 0.518 | 0.618 | 0.520 | 0.554 | 0.519 | 0.563 | 0.337 | 0.606 |
| S | 175.00 | 256.00 | 254.00 | 345.00 | 471.00 | 424.00 | 505.00 | 424.00 | 451.00 | 424.00 | 460.00 | 276.00 | 496.00 |
| Z value | 1.955 | 2.865 | 2.843 | 3.865 | 5.281 | 4.752 | 5.663 | 4.754 | 5.059 | 4.753 | 5.158 | 3.089 | 5.561 |
| p value | 0.051 | 0.004 | 0.004 | 0.000 | 0.000 | 0.000 | 0.000 | 0.000 | 0.000 | 0.000 | 0.000 | 0.002 | 0.000 |
| ACF | - 0.063 | - 0.001 | 0.064 | 0.179 | 0.520 | 0.390 | 0.600 | 0.506 | 0.501 | 0.469 | 0.587 | 0.168 | 0.641 |
| Sen slope | na | na | na | na | na | 0.023 | 0.030 | 0.024 | 0.023 | 0.025 | 0.030 | na | 0.026 |
| Northern Nigeria | | | | | | | | | | | | | |
| Danja | | | | | | | | | | | | | |
| τ | 0.192 | 0.233 | 0.423 | 0.427 | 0.457 | 0.471 | 0.393 | 0.206 | 0.392 | 0.435 | 0.346 | 0.442 | 0.442 |
| S | 157.00 | 191.00 | 347.00 | 350.00 | 474.00 | 385.00 | 322.00 | 168.00 | 321.00 | 356.00 | 284.00 | 141.00 | 362.00 |
| Z value | 1.752 | 2.134 | 3.886 | 3.920 | 4.190 | 4.314 | 3.606 | 1.877 | 3.595 | 3.988 | 3.179 | 1.573 | 4.055 |
| p value | 0.080 | 0.033 | 0.000 | 0.000 | 0.000 | 0.000 | 0.000 | 0.061 | 0.000 | 0.000 | 0.001 | 0.116 | 0.000 |
| ACF | - 0.07 | 0.33 | 0.413 | 0.386 | 0.499 | 0.486 | 0.376 | 0.481 | 0.313 | 0.549 | 0.398 | 0.081 | 0.719 |
| Sen slope | na | na | 0.061 | 0.055 | 0.068 | 0.053 | 0.035 | 0.012 | 0.023 | 0.055 | 0.068 | na | 0.048 |
| Faskari | | | | | | | | | | | | | |
| T | 0.213 | 0.231 | 0.448 | 0.443 | 0.423 | 0.505 | 0.403 | 0.217 | 0.405 | 0.468 | 0.376 | 0.196 | 0.000 |
| S | 174.00 | 189.00 | 368.00 | 363.00 | 347.00 | 414.00 | 330.00 | 177.00 | 331.00 | 382.00 | 308.00 | 161.00 | 370.00 |
| Z value | 1.944 | 2.112 | 4.122 | 4.067 | 3.887 | 4.639 | 3.696 | 1.978 | 3.708 | 4.282 | 3.449 | 1.797 | 4.147 |
| p value | 0.052 | 0.231 | 0.449 | 0.000 | 0.000 | 0.000 | 0.000 | 0.048 | 0.000 | 0.000 | 0.000 | 0.070 | 0.000 |
| ACF | - 0.002 | 0.341 | 0.44 | 0.389 | 0.415 | 0.501 | 0.428 | 0.446 | 0.331 | 0.561 | 0.46 | 0.128 | 0.732 |
| Sen slope | - | 0.069 | 0.059 | 0.054 | 0.064 | 0.046 | 0.032 | 0.012 | 0.020 | 0.050 | 0.067 | na | 0.045 |

τ is the Kendall rank correlation coefficient, S is the Kendall statistics, ACF is the autocorrelation coefficient, and Z and p values compare level of significance of Kendall statistics

however, the decrease is more significant and intense in the semi-arid regions than in the tropics.

SPIs of each study area are shown in Fig. 2. The SPIs of 41 years’ historical monthly rainfall in Tai ranged from - 3.28 to 4.44. Of a total of 492 months, 347 months’ rainfall data are within the normal range, while rainfall for 8, 13, and 36 months were within extremely dry, very dry, and moderately dry conditions, respectively (Fig. 2a). In Obio-Akpor, the same trend of SPIs was observed. A total of 343 monthly rainfall amounts were normal, and 9, 17, and 36 months’ rainfall data were within extremely dry, very dry, and moderately dry conditions, respectively (Fig. 2b).

On the contrary, the SPIs of historical rainfall in Danja ranged from - 3.14 to 4.61. The number of rainfall within the normal conditions is much lower (177), but rainfall amounts that occurred during 174 of 492 months are

within the extremely dry conditions (Fig. 5). Rainfall variabilities in Danja and Faskari are also closely related. Out of 492 monthly rainfall data, 222 are within the extremely dry conditions. This implies only 270-month experienced rainfall that can adequately replace lost humidity and soil moisture. Out of these 270 months, rainfalls experienced during 16 months were sparse and thus lead to very dry condition, 21 are within the moderately dry conditions, 185 within the normal condition, and only 7 fall within the very wet conditions (Fig. 2c and d). The SPIs of rainfall in Danja and Faskari give further credence to the incessant drought experienced in the semi-arid regions (Begizew 2021) as observed from the trend analysis.

Trends of minimum and maximum temperature averages in southern Nigeria were observed to increase significantly over the period studied. The historic monthly temperatures

Table 6 Averages of temperature indices between 1981 and 2021 in the four study areas

| Locations | TN90p (%) | TX90p (%) | TNx (°C) | TXx (°C) | TR25 (days) | SU35 (days) | TN10p (%) | TX10p (%) | TNn (°C) | TXn (°C) | TX15 (days) | TN10 (days) | DTR (°C) |
|------------|-----------|-----------|----------|----------|-------------|-------------|-----------|-----------|----------|----------|-------------|-------------|----------|
| Tai | 9.84 | 10.01 | 24.93 | 33.71 | 3.45 | 0.125 | 9.78 | 9.99 | 15.86 | 25.11 | 0.00 | 0.00 | 12.21 |
| Obio/Akpor | 9.84 | 10.01 | 24.89 | 33.50 | 3.30 | 0.025 | 9.77 | 12.13 | 15.74 | 25.27 | 0.00 | 0.00 | 6.72 |
| Danja | 10.03 | 10.10 | 24.68 | 39.42 | 1.20 | 63.03 | 9.79 | 10.02 | 8.59 | 23.32 | 0.00 | 11.2 | 18.06 |
| Faskari | 10.02 | 10.08 | 24.91 | 39.91 | 1.65 | 69.95 | 12.02 | 9.64 | 9.72 | 24.02 | 0.00 | 3.60 | 17.91 |

in both the tropics and semi-arid regions increased significantly for most months. In Obio-Akpor, only historic temperature of January increased mildly. However, in Tai and Obio-Akpor, the increases of temperature during the entire months were largely significant (Table 5). In Danja and Faskari, the historic temperature increased mildly in January and in Faskari, the increasing positive trends in temperature during January, February, and March were also observed to be mild (Table 5). These mild positive trends can be attributed to zero rainfall always experienced in the semi-arid regions during these months. These make the temperature perpetually high; only mild changes are thus experienced, annually. Total annual temperature also increased significantly. Evidenced significant temperature increases were attributed to depletion of ozone layer and climate change over the years (Tabari 2020; Clarke et al. 2022). These significant increases in temperature are in tandem with the observation of Alhaji et al. (2018) and Diagi et al. (2020). The maximum and average temperatures in southern Nigeria had significantly positive time series trends between 1984 and 2015 (Diagi et al. 2020).

Considering the temperature indices (Table 6) for comparison of average temperature between studied locations, the northern regions experienced warmer days and nights than the southern regions. In the semi-arid regions, highest maximum temperature ranged from 39.42 to 39.91, in contrast to a range of 33.50 to 33.71 in the tropics. The humid region experienced more days with minimum temperature greater than 25 °C in comparison with the semi-arid regions. The semi-arid regions however experienced higher number of summer days (63.03 to 68.95 days), when maximum temperatures are greater than 35 °C. Invariably, the semi-arid regions also experienced more cold days and therefore higher mean differences between the maximum and minimum temperatures (17.91 to 18.06) as compared to a range of 6.72 to 12.21 in the tropics (Table 6).

To further investigate the variabilities of rainfall and temperature, differences between monthly precipitation and evapotranspiration data fitted to a log-logistic distribution resulted in the SPEIs. Figure 3 shows the SPEIs of the study areas. Tai, Obio Akpor, Danja, and Faskari had 318, 298, 303, and 307 months classified as having normal differences between precipitation and evapotranspiration (which is largely influenced by temperature). Figure 3a to d depicts the SPEI of each study area indicated that mild but intermittent dryness (shown by the red colors) in the southern regions spread over the entire years of data. However, in the northern regions, dryness was concentrated and more intense in recent years, starting from around the year 2000 as shown in Fig. 3c and d. These are attributable to the significantly increasing temperature observed from the trend analysis.

Table 7 Trend analysis of soil moisture (0–5 cm) in LGAs of southern and northern Nigeria

| Parameters | Jan. | Feb. | Mar. | Apr. | May | Jun. | Jul. | Aug. | Sept. | Oct. | Nov. | Dec. | Annual |
|-------------------------|---------|---------|---------|---------|---------|---------|---------|---------|---------|---------|---------|---------|---------|
| Southern Nigeria | | | | | | | | | | | | | |
| Tai | | | | | | | | | | | | | |
| τ | -0.019 | 0.106 | 0.106 | -0.083 | -0.246 | -0.182 | -0.102 | 0.003 | 0.089 | -0.173 | 0.069 | 0.077 | -0.056 |
| <i>S</i> | -15.00 | 83.00 | 84.00 | -65.00 | -194.00 | -147.00 | -80.00 | 2.000 | 67.00 | -132.00 | 53.00 | 60.00 | -43.00 |
| <i>Z</i> value | -0.158 | 0.931 | 0.938 | -0.726 | -2.184 | -1.643 | -0.897 | 0.011 | 0.761 | -1.499 | 0.592 | 0.671 | -0.477 |
| <i>p</i> value | 0.874 | 0.352 | 0.348 | 0.468 | 0.029 | 0.100 | 0.370 | 0.991 | 0.447 | 0.134 | 0.554 | 0.502 | 0.633 |
| ACF | -0.216 | -0.233 | -0.367 | -0.238 | 0.305 | 0.316 | 0.058 | 0.021 | 0.268 | 0.257 | 0.136 | -0.041 | 0.200 |
| Sen slope | na | na | 0.001 | - | -0.001 | -0.133 | na | na | na | na | na | na | na |
| Obio Akpor | | | | | | | | | | | | | |
| τ | 0.029 | 0.062 | 0.076 | -0.190 | -0.283 | -0.230 | -0.138 | -0.052 | 0.032 | -0.158 | 0.005 | -0.025 | -0.137 |
| <i>S</i> | -23.00 | 49.00 | 60.00 | -151.00 | -226.00 | -184.00 | -109.00 | -41.00 | 25.00 | -121.00 | 4.00 | 20.00 | -106.00 |
| <i>Z</i> value | -0.249 | 0.542 | 0.668 | -1.692 | -2.536 | -2.062 | -1.221 | -0.452 | 0.273 | 1.373 | 0.034 | 0.215 | -1.197 |
| <i>p</i> value | 0.803 | 0.588 | 0.504 | 0.091 | 0.011 | 0.039 | 0.222 | 0.652 | 0.785 | 0.170 | 0.973 | 0.830 | 0.232 |
| ACF | -0.260 | -0.200 | -0.239 | 0.012 | 0.430 | 0.378 | 0.181 | 0.006 | 0.250 | 0.137 | 0.030 | -0.070 | 0.285 |
| Sen slope | na | na | Na | na | -0.002 | -0.003 | na | na | na | na | na | na | na |
| Northern Nigeria | | | | | | | | | | | | | |
| Danja | | | | | | | | | | | | | |
| τ | -0.299 | -0.294 | -0.319 | -0.260 | -0.308 | -0.347 | -0.239 | -0.168 | -0.266 | -0.244 | -0.248 | -0.260 | -0.275 |
| <i>S</i> | -241.00 | -235.00 | -256.00 | -205.00 | -248.00 | -278.00 | -191.00 | -135.00 | -212.00 | -198.00 | -200.00 | -209.00 | -222.00 |
| <i>Z</i> value | -2.702 | -2.639 | -2.873 | -2.311 | -2.781 | -3.122 | -2.143 | -1.510 | -2.383 | -2.216 | -2.241 | -2.342 | -2.487 |
| <i>p</i> value | 0.007 | 0.008 | 0.004 | 0.021 | 0.005 | 0.002 | 0.032 | 0.131 | 0.017 | 0.027 | 0.025 | 0.019 | 0.013 |
| ACF | 0.493 | 0.474 | 0.562 | 0.348 | 0.335 | 0.434 | 0.399 | 0.379 | 0.328 | 0.442 | 0.480 | 0.477 | 0.685 |
| Sen slope | -0.003 | -0.002 | -0.003 | -0.002 | -0.002 | -0.003 | -0.002 | -0.001 | -0.003 | -0.003 | -0.004 | -0.003 | -0.002 |
| Faskari | | | | | | | | | | | | | |
| τ | -0.302 | -0.301 | -0.346 | -0.295 | -0.334 | -0.405 | -0.242 | -0.188 | -0.259 | -0.216 | -0.229 | -0.248 | -0.330 |
| <i>S</i> | -241.00 | -240.00 | -277.00 | -236.00 | -267.00 | -325.00 | -193.00 | -148.00 | -207.00 | -173.00 | -185.00 | -200.00 | -263.00 |
| <i>Z</i> value | -2.707 | -2.497 | -3.112 | -2.649 | -2.999 | -3.650 | -2.167 | -1.665 | -2.323 | -1.939 | -2.071 | -2.240 | -2.957 |
| <i>p</i> value | 0.007 | 0.007 | 0.002 | 0.008 | 0.003 | 0.000 | 0.030 | 0.096 | 0.020 | 0.053 | 0.038 | 0.025 | 0.003 |
| ACF | 0.463 | 0.469 | 0.573 | 0.164 | 0.278 | 0.496 | 0.463 | 0.384 | 0.355 | 0.385 | 0.446 | 0.466 | 0.711 |
| Sen slope | -0.002 | -0.002 | -0.002 | na | na | -0.003 | -0.002 | -0.001 | -0.002 | -0.002 | -0.003 | -0.002 | -0.002 |

τ is the Kendall rank correlation coefficient, *S* is the Kendall statistics, ACF is the autocorrelation coefficient, *Z* and *p* values compare level of significance of Kendall statistics, and na means no value

Table 8 Trend analysis of root zone moisture (0–100 cm) in LGAs of southern and northern Nigeria

| Parameters | Jan. | Feb. | Mar. | Apr. | May | Jun. | Jul. | Aug. | Sept. | Oct. | Nov. | Dec. | Annual |
|-------------------------|---------|---------|---------|---------|---------|---------|---------|---------|---------|---------|---------|---------|---------|
| Southern Nigeria | | | | | | | | | | | | | |
| Tai | | | | | | | | | | | | | |
| τ | -0.026 | 0.066 | 0.095 | -0.057 | -0.228 | -0.201 | -0.110 | 0.022 | 0.067 | -0.138 | 0.037 | 0.095 | -0.073 |
| <i>S</i> | -21.00 | 52.00 | 74.00 | -46.00 | -182.00 | -160.00 | -87.00 | 17.00 | 51.00 | -101.00 | 29.00 | 76.00 | -56.00 |
| <i>Z</i> value | -0.226 | 0.576 | 0.830 | -0.507 | -2.042 | -1.813 | -0.972 | 0.182 | 0.572 | -1.167 | 0.319 | 0.846 | -0.629 |
| <i>p</i> value | 0.821 | 0.565 | 0.407 | 0.612 | 0.041 | 0.070 | 0.331 | 0.856 | 0.567 | 0.243 | 0.750 | 0.398 | 0.530 |
| ACF | -0.182 | -0.242 | -0.343 | -0.251 | 0.291 | 0.344 | 0.046 | 0.021 | 0.299 | 0.281 | 0.190 | 0.006 | 0.215 |
| Sen slope | na | na | na | na | na | -0.002 | na | na | na | na | na | na | na |
| Obio Akpor | | | | | | | | | | | | | |
| τ | -0.045 | 0.079 | 0.067 | -0.155 | -0.275 | 0.248 | -0.120 | -0.050 | 0.059 | -0.131 | 0.046 | 0.049 | -0.146 |
| <i>S</i> | -35.00 | 61.00 | 52.00 | -122.00 | -222.00 | -200.00 | 94.00 | 39.00 | 45.00 | -97.00 | 36.00 | 39.00 | -115.00 |
| <i>Z</i> value | -0.388 | 0.682 | 0.579 | 1.371 | -2.487 | -2.240 | -1.055 | -0.431 | 0.503 | -1.111 | 0.397 | 0.430 | -1.290 |
| <i>p</i> value | 0.698 | 0.495 | 0.563 | 0.170 | 0.013 | 0.025 | 0.292 | 0.666 | 0.615 | 0.267 | 0.691 | 0.667 | 0.197 |
| ACF | -0.246 | -0.246 | -0.331 | -0.048 | 0.410 | 0.386 | 0.169 | -0.036 | 0.159 | 0.125 | 0.025 | 0.080 | 0.308 |
| Sen slope | na | na | na | na | -0.002 | -0.003 | na | na | na | na | na | na | na |
| Northern Nigeria | | | | | | | | | | | | | |
| Danja | | | | | | | | | | | | | |
| τ | -0.293 | -0.283 | -0.337 | -0.263 | -0.277 | -0.359 | -0.214 | -0.154 | -0.023 | -0.252 | -0.242 | 0.251 | -0.280 |
| <i>S</i> | -233.00 | 220.00 | -255.00 | -196.00 | -215.00 | -284.00 | -171.00 | -123.00 | -198.00 | 202.00 | -192.00 | -203.00 | -222.00 |
| <i>Z</i> value | -2.619 | -2.485 | -2.910 | -2.243 | -2.432 | -3.200 | -1.917 | -1.377 | -2.218 | -2.266 | -2.157 | -2.27 | -2.496 |
| <i>p</i> value | 0.009 | 0.013 | 0.004 | 0.025 | 0.015 | 0.001 | 0.055 | 0.168 | 0.252 | 0.023 | 0.031 | 0.023 | 0.013 |
| ACF | 0.569 | 0.542 | 0.597 | 0.416 | 0.388 | 0.515 | 0.392 | 0.361 | 0.344 | 0.440 | 0.483 | 0.514 | 0.601 |
| Sen slope | -0.001 | -0.001 | -0.001 | -0.000 | -0.001 | -0.002 | -0.002 | -0.001 | -0.002 | -0.003 | -0.003 | -0.002 | -0.002 |
| Faskari | | | | | | | | | | | | | |
| τ | -0.286 | -0.311 | -0.323 | -0.296 | -0.347 | -0.410 | 0.024 | -0.191 | -0.257 | -0.228 | -0.228 | -2.068 | -0.299 |
| <i>S</i> | -224.00 | -237.00 | -228.00 | -211.00 | -273.00 | -327.00 | -200.00 | -153.00 | -207.00 | -183.00 | -183.00 | -184.00 | -237.00 |
| <i>Z</i> value | -2.525 | -2.695 | -2.696 | -2.485 | -3.077 | -3.675 | -2.245 | -1.713 | -2.319 | -2.051 | -2.050 | -2.068 | -2.665 |
| <i>p</i> value | 0.012 | 0.007 | 0.007 | 0.013 | 0.002 | 0.000 | 0.024 | 0.087 | 0.020 | 0.040 | 0.040 | 0.039 | 0.008 |
| ACF | 0.524 | 0.507 | 0.558 | 0.151 | 0.389 | 0.539 | 0.451 | 0.372 | 0.370 | 0.417 | 0.470 | 0.491 | 0.604 |
| Sen slope | -0.001 | -0.001 | -0.000 | na | -0.001 | -0.002 | -0.002 | -0.001 | -0.002 | -0.002 | -0.002 | -0.002 | -0.001 |

τ is the Kendall rank correlation coefficient, *S* is the Kendall statistics, ACF is the autocorrelation coefficient, *Z* and *p* values compare level of significance of Kendall statistics, and na means no value

Fig. 2 The SPIs for precipitation in Tai, Obio-Akpor, Danja, and Faskari, respectively

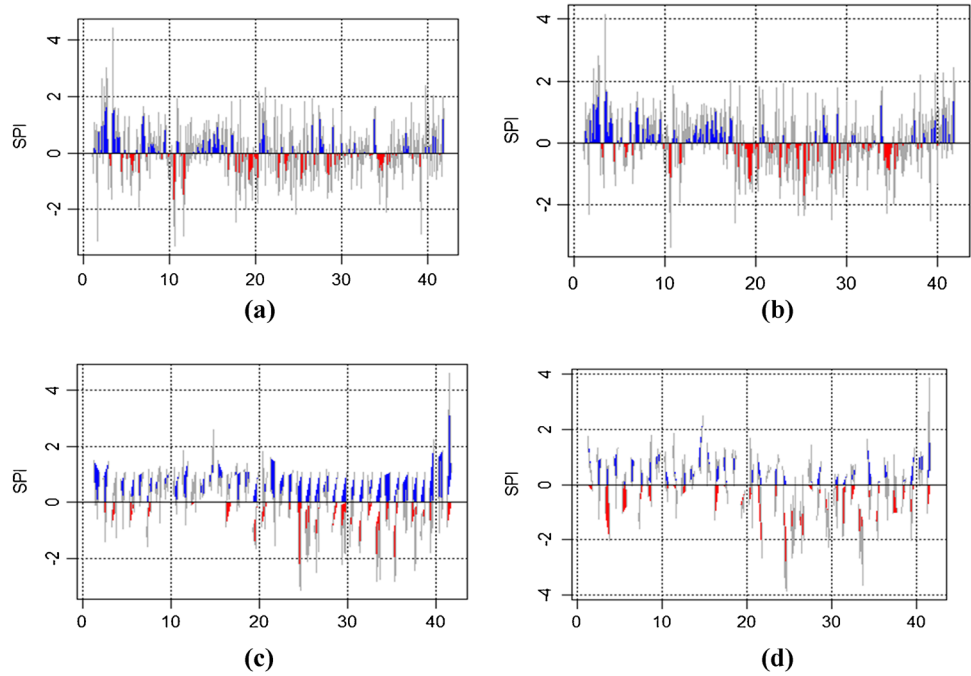
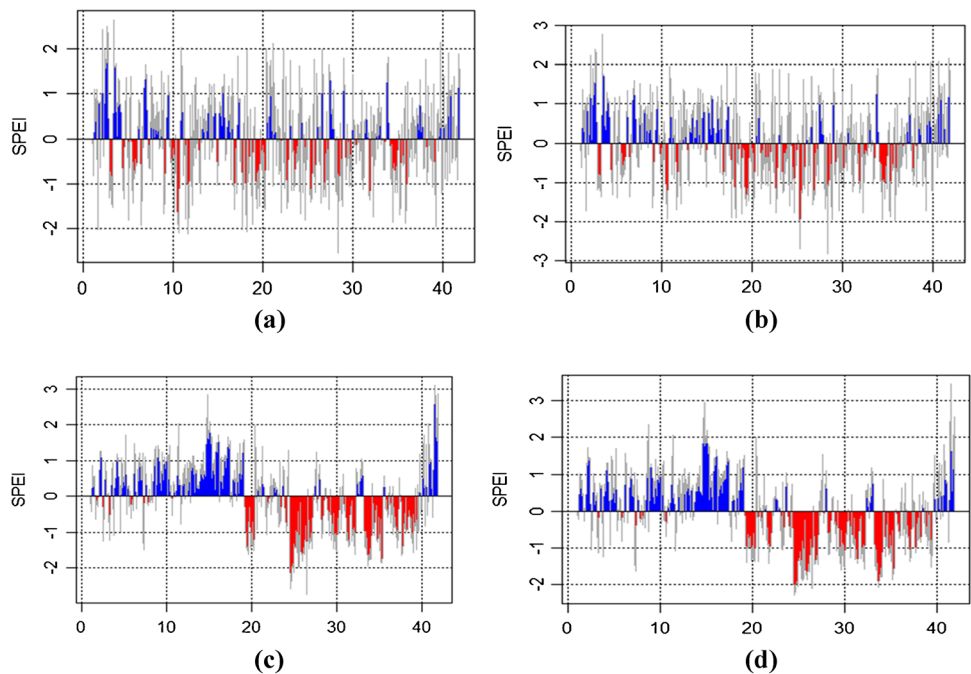


Fig. 3 The SPEIs of differences between precipitation and evapotranspiration in Tai, Obio-Akpor, Danja, and Faskari, respectively



The SPEI as an index seemed not to reflect the true state of wetness and dryness in the regions; PDSI was thus used to further explain the state of drought and wetness from historical temperature and precipitation observations. PDSIs of the study areas are shown in Fig. 4. In Tai, PDSIs ranged from -4.10 to 9.89 (Fig. 4a). Based on resulting PSDIs of 41-year (492 months) observations, extreme droughts (ED) were experienced for 2 months, severe drought (SD) for 27 months, moderate drought (MD) for 68 months, mild drought

(MID) for 283 months, slight wetness (SW) for 57 months, moderate wetness (MW) for 21 months, very wet (VW) conditions for 7 months, and extremely wet (EW) conditions for 27 months (Fig. 4a). In the same vein, PDSIs for Obio-Akpor ranged from -4.55 to 9.05 . ED, SD, MD, MID, SW, MW, and VW were experienced for 3, 41, 76, 214, 84, 36, and 26 months, in the same order (Fig. 4b). In comparison with PDSIs of the semi-arid regions, the humid region experienced lesser months of extreme, severe, and moderate drought, but

Fig. 4 The PDSI of precipitation and evapotranspiration in Tai, Obio-Akpor, Danja, and Faskari, respectively

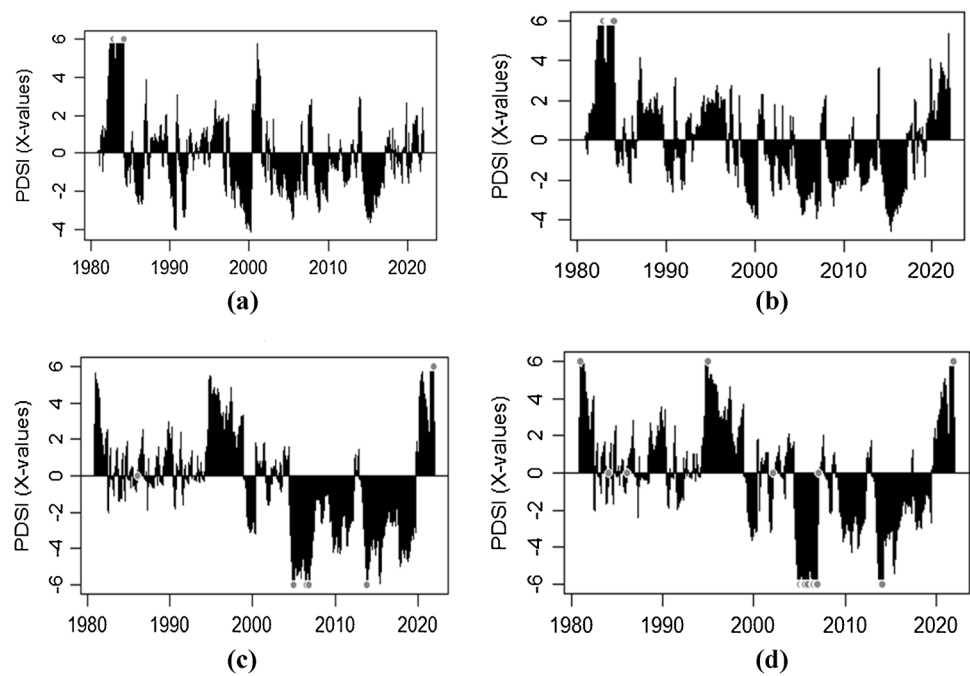
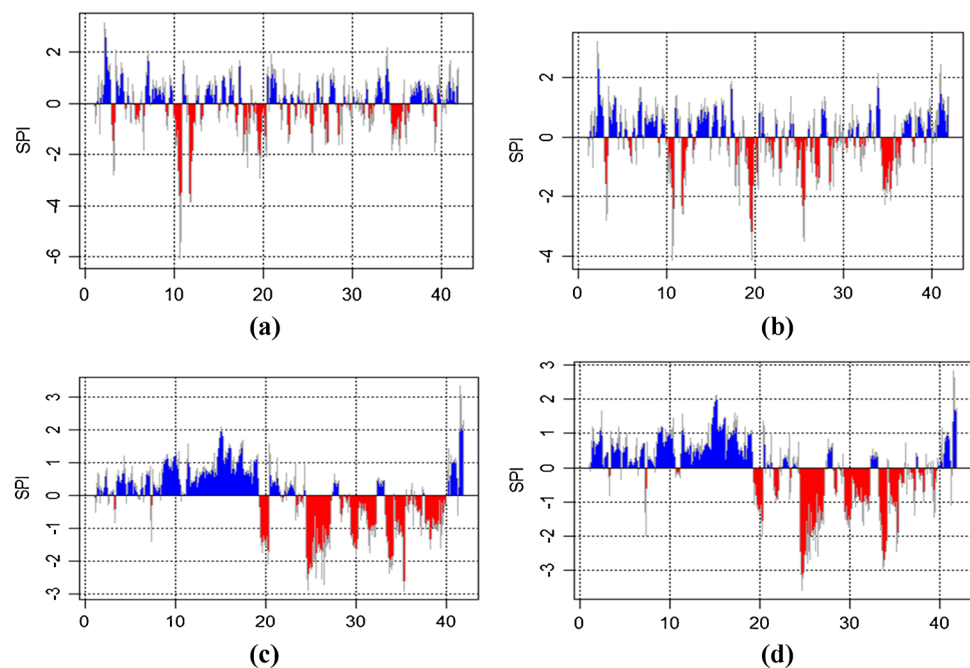


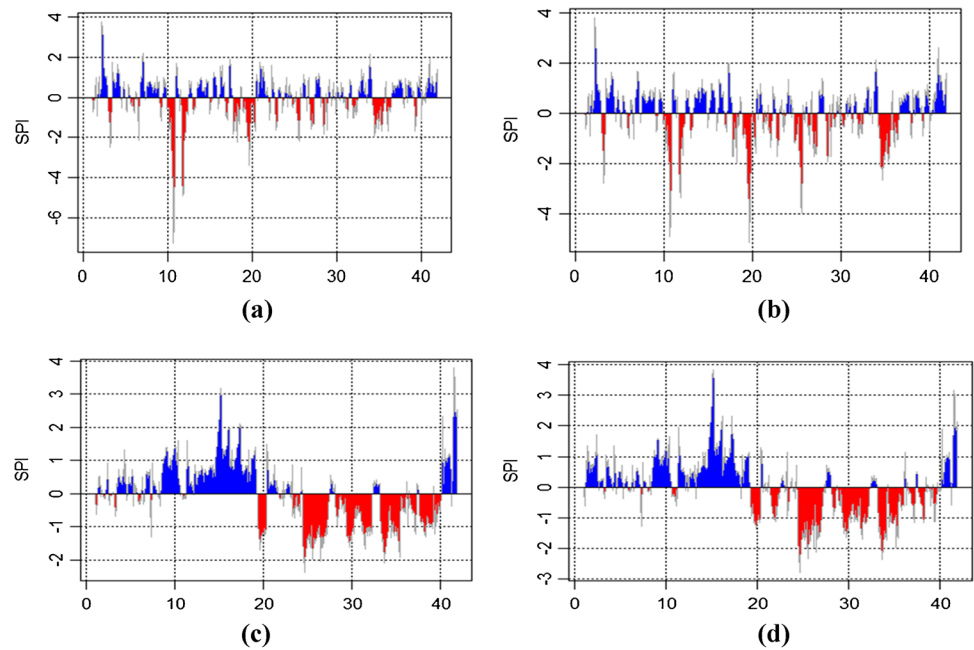
Fig. 5 The SPI for top soil moisture (0–5 cm) for Tai, Obio-Akpor, Danja, and Faskari, respectively



more periods of wetness than the semi-arid regions. The semi-arid regions were also observed to have wider ranges of PDSIs. PDSIs of Danja and Faskari ranged from -6.56 to 16.92 (Fig. 4c) and -8.15 to 9.55 (Fig. 4d), respectively. In Danja and Faskari, the 492 months studied are arranged in descending order of number of months that experienced

each condition. For Danja, MID (194) > ED (60) > MD (52) > SW (51) > SD (47) > EW (38) > MW (29) > VW (21). For Faskari, MID (200) > SW (58) > MD (52) > SD (41) > EW (40) > ED (39) > MW (38) > VW (24). Generally, it has been established that the semi-arid regions experienced more periods of drought than the southern region.

Fig. 6 The SPI for top soil moisture (0–100 cm) for Tai, Obio-Akpor, Danja, and Faskari, respectively



Effects of decreasing precipitation and increasing temperature on the trends and variabilities of soil moisture

Trends of moisture in the top soil (0–5 cm) and subsoil (0–100 cm), and below the soil surface are presented on Tables 7 and 8, respectively. The monthly top soil and subsoil moistures in the south generally show mild downward trends. The total annual top soil and subsoil moistures also decreased mildly over the 41 years studied. In Tai, February, March (subsoil), August, September, November, and December (subsoil) show mildly positive trend. On the contrary, May and June (subsoil) had significantly negative trend (Tables 7 and 8). In Obio-Akpor, soil moisture trends were also mildly positive, during January (topsoil), February, March, September, November, and December (subsoil). The mild positive trends were observed to occur during non-peak rainy periods, and these may be attributable to inadequate rainfall, which makes most water from such rainfall events to satisfy all other statutory demand such as evaporation, transpiration, infiltration, interception, and percolation (Langat et al. 2017; Alahacoon and Edirisinghe 2021). Such mild positive trend may also be due to capillary rise from the groundwater table or even delayed movement of subsurface flow from during peak rainy seasons (Bousbih et al. 2018). Furthermore, in Obio-Akpor, the topsoil moisture during May and June decreased significantly. The subsoil moisture in May decreased significantly, while the same had significant increase in June. The trend pattern obtained for the topsoil and subsoil moisture closely fashioned after those obtained for rainfall. This further reinforces the claim that soil moisture storage is influenced by the rainfall amount (Hartzell et al. 2017; Akbar et al. 2018). Investigation

from drought indices revealed that the SPIs of topsoil and subsoil moistures ranged from -6.08 to 3.17 (Fig. 5a) and -7.27 to 3.79 (Fig. 6a), respectively, in Tai, and -4.13 to 3.22 (Fig. 5b) and -5.14 to 3.83 (Fig. 6b), respectively, in Obio-Akpor. The wide range of indices show the effect of dry and wet seasons on soil moisture (Emerson and Traver 2008). During the wet season, the soil is excessively wet, but such wetness is used up to satisfy evapotranspiration and atmospheric water needs during short duration drought (Welch et al. 2018; Dunning et al. 2018).

Several factors accompany climate change, including non-stationary precipitation, heightened extreme events like floods, droughts, and heatwaves, as well as increases in sea surface temperature and soil moisture loss, which have severe effects on crop performances (Mathivha and Mbatha 2022). Contrary to trends of topsoil and subsoil moisture in the humid southern region, soil moisture regimes in the semi-arid regions significantly decreased continuously. The total annual topsoil and subsoil moistures in the northern region decreased significantly. In Danja, the topsoil moisture decreased significantly through all the months except August which had just mild decrease. At the root zone (subsoil) the soil moistures for July, August, and September also decreased mildly (Tables 6 and 7). The negative Sen's slope obtained from the MMK tests further reinforced claims from the significant moisture decreases from the MK tests. In Faskari, the topsoil and subsoil moistures decreased significantly for all months, except in August and October when the topsoil moisture had only mild decrease. These significant decreases in top and subsoil moistures can be attributed to low and decreasing precipitation and also increasing temperature which causes high evapotranspiration (Asoka et al. 2017).

The increasingly reducing precipitation and consistent significant increase in temperature had adverse effect on the storage of soil moisture at different depths (Konapala et al. 2020). This would invariably have negative influence on agricultural production which depends on the constant supply of soil moisture for increased productivity (Ford and Quiring 2019; Rigden et al. 2020). The need for proper water management, water conservation, soil water conservation, and irrigation for sustainable food production cannot be overemphasized for increased soil moisture storage and improved crop water productivity (Yu et al. 2018; Sadeghi et al. 2019). Assessment of soil moisture in the semi-arid regions in drought indicial terms revealed the SPI of topsoil and subsoil moistures ranged from -2.92 to 3.34 (Fig. 5c) and -2.37 to 3.80 (Fig. 6c), respectively, in Danja and -3.57 to 2.83 (Fig. 5d) and -2.79 to 3.84 (Fig. 6d), respectively, in Faskari. As depicted by the SPEIs of precipitation of the semi-arid region, the SPIs of both top soil and sub soil moisture also followed the same patterns. In the northern regions, dryness has been concentrated and more intense in recent years (as shown by the red colors), starting from around the year 2000 as shown in Fig. 5c, d, Fig. 6c, and d. Such increasing drying can be attributed to issues linked to climate change and global warming (Hao et al. 2018; Schimel 2018; DeSoto et al. 2020). The minimal range of indices (SPI) in comparison to those obtained in the southern part implies there are minimal differences between stored soil moisture during wet and dry seasons (Cheng et al. 2015; Babaeian et al. 2019). Such minimal differences are attributable to small precipitation amount and excessive evaporation, resulting from high temperature (Konapala et al. 2020).

Kew et al. (2021) however contradicted some of the findings of this current study, noting no discernible trend in soil moisture and precipitation data from 1900 to 2018 in eastern Africa. Their study highlighted precipitation as the primary influencer of soil moisture variability, particularly in water-scarce regions, with evaporative demand and temperature showing weaker correlations. The claims that precipitation had great influence on soil moisture trend are in tandem with the findings of this study. The trends of evaporative demand and local temperatures were however positive. The study concluded that the impact of rising temperatures on soil moisture in eastern Africa was limited, though it recommended that precipitation analysis can comfortably replace soil moisture analysis for drought studies. Conversely, Wu et al. (2021) identified a strong correlation between soil moisture dynamics and ocean surface temperature when assessing regional spatiotemporal variations of drought in Guangxi, China. Additionally, Kelley et al. (2015) linked changes in precipitation in Syria to rising mean sea level pressure in the Eastern Mediterranean. They attributed decreased precipitation to both natural causes and long-term drying trends associated

with warming, thus, contributing significantly to soil moisture reduction (Kelley et al. 2015).

In alignment with the soil moisture trends identified in our current study, Almendra-Martin et al. (2021) highlighted the prevalence of a negative trend in soil moisture data retrieved from the Lisaflood and ER5-Land databases for the Iberian Peninsula. These negative trends were found to escalate with higher clay contents and persisted over a span of 10 months, coinciding with the typical growing seasons of crops in the region. However, the study also noted positive trends in soil moisture for 2 months (Almendra-Martin et al. 2021). Invariably, the hypothesis set for this study is true that the trends and variability of precipitation and temperature are determinants of the trends and variability of soil moisture in southern and northern Nigeria.

Conclusion

This study examined and compared the temporal trends and variabilities of monthly and annual rainfall, temperature, and soil moisture in southern and northern Nigeria, over the observation period 1981–2021. Over those four decades, precipitation as rainfall has had slight decrease in southern Nigeria, in contrast to northern Nigeria which had experienced very significant decrease over the same period. Both southern and northern Nigeria experienced significant temperature increase over the four decades. However, temperature indices including hottest days (TXx), summer day (SU35), and diurnal temperature range (DTR), among others, indicated northern Nigeria experienced more extreme temperature increase than southern Nigeria. The continuous increase in temperature and decrease in precipitation are attributable to climate change and global warming caused by ozone layer depletion. Drought indices including standardize precipitation index (SPI), standardized precipitation evaporation index (SPEI), and Palmer drought severity index (PDSI) gave credence to the fact that northern Nigeria experienced more drought period over the four decades than southern Nigeria. As a result of low precipitation and high temperature, soil moisture storage in northern Nigeria reduced significantly over the four decades, while soil moisture reduction in southern Nigeria was mild.

The trends and variabilities of precipitation and soil moisture from the MK and SPI tests were observed to be in close tandem for the southern and northern divides of Nigeria. The increase in temperature trends and resultant decrease in soil moisture trends could also imply the influence of temperature on soil moisture. The pronounced effects of precipitation and temperature trends on topsoil and subsoil moisture trends therefore require more efforts geared toward climate smart agriculture, climate smart water management,

soil moisture conservation, and provision of more irrigation schemes in both divides of the country but most especially in northern Nigeria. These would enhance sustainable agricultural food production and food security in the face of lingering fresh water scarcity. This study has identified the monthly trend and variability of precipitation, temperature, and soil moisture conditions. The study can be of immense help to farmers, foresters, agriculturist, tourism industry, and environmentalist, among others, in coping with climate issues more effectively and efficiently. It is recommended that climate smart agriculture, which promotes soil water conservation by preventing excessive soil moisture losses, should be practiced and enabled in the study area. Further research on the effects of soil temperature on soil moisture losses and effects of climate smart practices on soil moisture conservation and crop yield is also recommended.

Author contribution Conceptualization, data collection, data curation, data analysis, and original write-up: B. F. Sasanya. Introduction, methodology, and proofreading: A. Ademola. Supervision, writing, review, and editing: S.O. Adesogan. The author and co-author agreed to publish this version of the research article.

Data availability The raw data are available at reasonable request from the authors.

Declarations

Ethics approval All authors have read, understood, and have complied as applicable with the statement on “Ethical responsibilities of Authors” as found in the Instructions for Authors and are aware that with minor exceptions, no changes can be made to authorship once the paper is submitted.

Consent to participate Not applicable.

Consent for publication Not applicable.

Conflict of interest The authors declare no competing interests.

References

- Aamir E, Khan A, Abubakar Tariq M (2022) The influence of teleconnections on the precipitation in Baluchistan. *Atmosphere* 2022(13):1001. <https://doi.org/10.3390/atmos13071001>
- Adakayi P, Oche C, Ishaya S (2016) Assessment of the patterns of rainfall in northern Nigeria. *Ethiopian J Environ Stud Manag* 9(5). <https://doi.org/10.4314/ejesm.v9i5.3>
- Adesogan SO, Sasanya BF (2021) Water availability investigation and assessment in South - Western Nigeria. *Int J Energy Water Resour*:0123456789. <https://doi.org/10.1007/s42108-021-00136-2>
- Adesogan SO, Sasanya BF (2023) Efficiency of indirect and estimated evapotranspiration methods in South Western Nigeria. *Int J Hydrol Sci Technol* 15(1):64–77. <https://doi.org/10.1504/IJHST.2021.10041388>
- Ahmad MI, Sinclair CD, Werritty A (1988) Log-logistic flood frequency analysis. *J Hydrol* 98(3–4). [https://doi.org/10.1016/0022-1694\(88\)90015-7](https://doi.org/10.1016/0022-1694(88)90015-7)
- Akbar R, Short Gianotti D, McColl KA, Haghghi E, Salvucci GD, Entekhabi D (2018) Hydrological storage length scales represented by remote sensing estimates of soil moisture and precipitation. *Water Resources Research*. 54(3): 1476–1492. <https://doi.org/10.1002/2017WR021508>
- Alahacoon N, Edirisinghe M (2021) Spatial variability of rainfall trends in Sri Lanka from 1989 to 2019 as an indication of climate change. *ISPRS Int J Geo Inf* 2021(10):84. <https://doi.org/10.3390/ijgi10020084>
- Alhaji UU, Yusuf AS, Edet CO, Oche CO, Agbo EP (2018) Trend analysis of temperature in Gombe State using Mann Kendall trend test. *J Sci Res Rep* 20(3). <https://doi.org/10.9734/jsrr/2018/42029>
- Ali S, Ghosh NC, Singh R (2010) Rainfall–runoff simulation using a normalized antecedent precipitation index. *Hydrol Sci J* 55(2). <https://doi.org/10.1080/02626660903546175>
- Alley WM (1984) The Palmer drought severity index: limitations and assumptions. *J Clim Appl Meteorol* 23(7):1100–1109. [https://doi.org/10.1175/1520-0450\(1984\)023<1100:TPDSSL>2.0.CO;2](https://doi.org/10.1175/1520-0450(1984)023<1100:TPDSSL>2.0.CO;2)
- Al-timimi YK, Osamah A (2016) Comparative study of four meteorological drought indices in Iraq. *IOSR J Appl Phys* 8(5):76–84. <https://doi.org/10.9790/4861-0805037684>
- Almendra-Martín L, Martínez-Fernández J, González-Zamora Á, Benito-Verdugo P, Herrero-Jiménez CM (2021) Agricultural drought trends on the Iberian Peninsula: An analysis using modeled and reanalysis soil moisture products. *Atmosphere*. 12(2):236. <https://doi.org/10.3390/atmos12020236>
- Anil AP, Ramesh H (2017) Analysis of climate trend and effect of land use land cover change on Harangi streamflow, South India: a case study. *Sustain Water Resour Manag* 3(3):257–267. <https://doi.org/10.1007/s40899-017-0088-5>
- Asoka A, Gleeson T, Wada Y, Mishra V (2017) Relative contribution of monsoon precipitation and pumping to changes in groundwater storage in India. *Nature Geoscience*. 10(2):109–117. <https://doi.org/10.1038/ngeo2869>
- Asfaw A, Simane B, Hassen A, Bantider A (2018) Variability and time series trend analysis of rainfall and temperature in northcentral Ethiopia: a case study in Woleka sub-basin. *Weather Clim Extrem* 19:29–41. <https://doi.org/10.1016/j.wace.2017.12.002>
- Babaeian E, Sadeghi M, Jones SB, Montzka C, Vereecken H, Tuller M (2019) Ground, proximal and satellite remote sensing of soil moisture. *Rev Geophys* 57(2):530–616. <https://doi.org/10.1029/2018rg00061>
- Begizew G (2021) Agricultural production system in arid and semi-arid regions. *Int J Agric Sci Food Technol* 7(2):234–244. <https://doi.org/10.17352/2455-815x.000113>
- Bhuiyan MDI, Islam MM, Bhuiyan MEK (2018) A trend analysis of temperature and rainfall to predict climate change for Northwestern Region of Bangladesh. *Am J Clim Chang* 07(02):115–134. <https://doi.org/10.4236/ajcc.2018.72009>
- Bong CHJ, Richard J (2020) Drought and climate change assessment using standardized precipitation index (SPI) for Sarawak River Basin. *J Water Clim Change* 11(4):956–965. <https://doi.org/10.2166/wcc.2019.036>
- Bousbih S, Zribi M, El Hajj M, Baghdadi N, Lili-Chabaane Z, Gao Q, Fanise P (2018) Soil moisture and irrigation mapping in a semi-arid region, based on the synergetic use of Sentinel-1 and Sentinel-2 Data. *Remote Sens* 10(12):1953. <https://doi.org/10.3390/rs10121953>
- Cheng S, Guan X, Huang J, Ji F, Guo R (2015) Long-term trend and variability of soil moisture over East Asia. *J Geophys Res Atmos* 120(17):8658–8670. <https://doi.org/10.1002/2015jd023206>
- Clarke B, Otto F, Stuart-Smith R, Harrington L (2022) Extreme weather impacts of climate change: an attribution perspective. *Environ Res: Climate* 1(1):012001. <https://doi.org/10.1088/2752-5295/ac6e7d>
- DeSoto L, Cailleret M, Sterck F, Jansen S, Kramer K, Robert EMR, Aakala T et al (2020) Low growth resilience to drought is related

- to future mortality risk in trees. *Nat Commun* 11(1):545. <https://doi.org/10.1038/s41467-020-14300-5>
- Diagi BE, Nwaerema P, Ajiere S (2020) Trend analysis of maximum and minimum temperature over Ebonyi State, Nigeria. *Soc Sci Humanit Sustain Res* 1(1):36–47. <https://doi.org/10.22158/sshsr.v1n1p36>
- Dunning CM, Black E, Allan RP (2018) Later wet seasons with more intense rainfall over Africa under future climate change. *J Clim* 31(23):9719–9738. <https://doi.org/10.1175/jcli-d-18-0102.1>
- Emerson CH, Traver RG (2008) Multiyear and seasonal variation of infiltration from storm-water best management practices. *J Irrig Drain Eng* 134(5):598–605. [https://doi.org/10.1061/\(asce\)07](https://doi.org/10.1061/(asce)07)
- Espinoza-Dávalos GE, Arctur DK, Teng W, Maidment DR, García-Martí I, Comair G (2015) Studying soil moisture at a national level through statistical analysis of NASA NLDAS data. *J Hydroinf* 18(2):277–287. <https://doi.org/10.2166/hydro.2015.23>
- Eze JN (2018) Drought occurrences and its implications on the households in Yobe state, Nigeria. *Geoenviron Disasters* 5, 18(1). <https://doi.org/10.1186/s40677-018-0111-7>
- Feng X, Porporato A, Rodriguez-Iturbe I (2013) Changes in rainfall seasonality in the tropics. *Nat Clim Chang* 3(9):811–815. <https://doi.org/10.1038/nclimate1907>
- Ford TW, Quiring SM (2019) Comparison of contemporary in situ, model, and satellite remote sensing soil moisture with a focus on drought monitoring. *Water Resources Research*. 55(2):1565–1582. <https://doi.org/10.1029/2018WR024039>
- Gebrechorkos SH, Hülsmann S, Bernhofer C (2019) Changes in temperature and precipitation extremes in Ethiopia, Kenya, and Tanzania. *Int J Climatol* 39(1):18–30. <https://doi.org/10.1002/joc.5777>
- Goswami BN, Venugopal V, Sangupta D, Madhusoodanan MS, Xavier PK (2006) Increasing trend of extreme rain events over India in a warming environment. *Science* 314(5804):1442–1445. <https://doi.org/10.1126/science.1132027>
- Hao Z, Singh VP, Xia Y (2018) Seasonal drought prediction: advances, challenges, and future prospects. *Rev Geophys* 56(1):108–141. <https://doi.org/10.1002/2016rg000549>
- Hartzell S, Bartlett MS, Porporato A (2017) The role of plant water storage and hydraulic strategies in relation to soil moisture availability. *Plant Soil* 419(1–2):503–521. <https://doi.org/10.1007/s11104-017-3341-7>
- Ibubuchi CC, Abu I (2023) Rainfall variability patterns in Nigeria during the rainy season. *Sci Rep* 13:7888
- Kelley CP, Mohtadib S, Canec MA, Seager R, Kushnir Y (2015) Climate change in the fertile crescent and implications of the recent Syrian drought. *PNAS* 112(11):3241–3246. <https://doi.org/10.1073/pnas.1421533112>
- Kew SF, Philip SY, Hauser M, Hobbins M, Wanders N, Oldenborgh GJ, Wiel K, Veldkamp TIE, Kimutai J, Funk C, Otto FEL (2021) Impact of precipitation and increasing temperatures on drought trends in eastern Africa. *Earth Syst Dynam* 12:17–35. <https://doi.org/10.5194/esd-12-17-2021>
- Khavse R, Deshmukh R, Manikandan N, Chaudhary JL, Kaushik D, Gandhi I, Viswadhylaya K, Raipur CG (2015) Statistical Analysis of Temperature and Rainfall Trend in Raipur District of Chhattisgarh. *Curr World Environ* 10(1):305–312
- Konapala G, Mishra AK, Wada Y, Mann ME (2020) Climate change will affect global water availability through compounding changes in seasonal precipitation and evaporation. *Nat Commun* 11(1):3044. <https://doi.org/10.1038/s41467-020-16757-w>
- Langat P, Kumar L, Koech R (2017) Temporal variability and trends of rainfall and streamflow in Tana River Basin, Kenya. *Sustainability* 9(11):1963. <https://doi.org/10.3390/su9111963>
- Lema MA, Majule AE (2009) Impacts of climate change, variability and adaptation strategies on agriculture in semi arid areas of Tanzania: the case of Manyoni District in Singida Region, Tanzania. *Afr J Environ Sci Technol* 3(8):206–218. <https://doi.org/10.5897/ajest09.099>
- Limsakul A (2020) Trends in Thailand's extreme temperature indices during 1955–2018 and their relationship with global mean temperature change. *Appl Environ Res* 42(2):94–107. <https://doi.org/10.35762/AER.2020.42.2.8>
- Mahajan DR, Dodamani BM (2016) Spatial and temporal drought analysis in the Krishna river basin of Maharashtra, India. *Cogent Eng* 3(1):1185926. <https://doi.org/10.1080/23311916.2016.1185926>
- Mathivha F, Mbatha N (2022) Comparison of long-term changes in non-linear aggregated drought index calibrated by MERRA–2 an NDII soil moisture proxies. *Water* 2022(14):26. <https://doi.org/10.3390/w14010026>
- McKee TB, Doesken NJ, Kleist J (1993) The relationship of drought frequency and duration to time scales. In *Proceedings of the 8th Conference on applied climatology* 17(22):179–183
- Nath H, Adhikary SK, Nath S, Kafy AA, Islam ARMT, Alsulamy S, Khedher KM, Shohan AAA (2024) Long-term trends and spatial variability in rainfall in the southeast region of Bangladesh: implication for sustainable water resources management. *Theoretical and Applied Climatology*:1–25. <https://doi.org/10.1007/s00704-024-04843-8>
- Ndlovu MS, Demlie M (2020) Assessment of meteorological drought and wet conditions using two drought indices across Kwazulu-Natal province, South Africa. *Atmosphere* 11(6):623. <https://doi.org/10.3390/atmos11060623>
- Nury AH, Hasan K, Dustegir M, Alam MJ (2017) Drought assessment using standardised precipitation evaporation index and its association with southern oscillation index in the Northwestern Bangladesh. *Int J Water* 11(2):132–158
- O'Brien NL, Burn DH, Annable WK, Thompson PJ (2021) Trend detection in the presence of positive and negative serial correlation: a comparison of block maxima and peaks-over-threshold data. *Water Resour Res* 57:e2020WR028886. <https://doi.org/10.1029/2020wr028886>
- Ogunrinde AT, Oguntunde PG, Olasehinde DA, Fasinmirin JT, Akinwumiju AS (2020) Drought spatiotemporal characterization using self-calibrating Palmer drought severity index in the northern region of Nigeria. *Results Eng* 5:100088. <https://doi.org/10.1016/j.rineng.2019.100088>
- Oufrih O, Elouissi A, Benzater B (2023) Trend assessment by the Mann-Kendall test and the innovative trend analysis method (North-West Algeria). *GeoSci Eng* 69(2):186–233. <https://doi.org/10.35180/gse-2023-0099>
- Pal AB, Khare D, Mishra PK, Singh L (2017) Trend analysis of rainfall, temperature and runoff data: a case study of Rangoon Watershed in Nepal. *Int J Stud Res Technol Manag* 5(3):21–38. <https://doi.org/10.18510/ijstrtm.2017.535>
- Palmer, WC (1965). *Meteorological Drought*. In U.S. Weather Bureau, Res. Pap. No. 45 (p. 58). <https://www.ncdc.noaa.gov/temp-and-precip/drought/docs/palmer.pdf>
- Patel NR, Anapashsha R, Kumar S, Saha SK, Dadhwal VK (2008) Assessing potential of MODIS derived temperature/vegetation condition index (TVDI) to infer soil moisture status. *Int J Remote Sens* 30, 23(1):–39. <https://doi.org/10.1080/01431160802108497>
- Paul JN, Katre P, Shori A (2023) Long term trend analysis of annual and seasonal rainfall for upstream of ravishanakar sagar reservoir. SSRN preprint. <https://doi.org/10.2139/ssrn.4603494>
- Revadekar JV, Kothawale DR, Patwardhan S, Kolli R (2012) About the observed and future changes in temperature extremes over India about the observed and future changes in temperature. *Nat Hazards* 60:1133–1155. <https://doi.org/10.1007/s11069-011-9895-4>
- Rigden AJ, Mueller ND, Holbrook NM, Pillai N, Huybers P (2020) Combined influence of soil moisture and atmospheric

- evaporative demand is important for accurately predicting US maize yields. *Nat Food* 1(2):127–133. <https://doi.org/10.1038/s43016-020-0028-7>
- Sadeghi M, Ebtehaj A, Crow WT, Gao L, Purdy AJ, Fisher JB, Babaeian E, Tuller M (2019) Global estimates of land surface water fluxes from SMOS and SMAP satellite soil moisture data. *J Hydrometeorol* 21(2):241–253. <https://doi.org/10.1175/jhm-d-19-0150>
- Salameh AAM, Gámiz-Fortis SR, Castro-Díez Y, Hammad AA, Esteban-Parra MJ (2019) Spatio-temporal Analysis for extreme temperature indices over Levant región. *Int J Climatol*. <https://doi.org/10.1002/joc.6171>
- Salameh AAM, Ojeda MG, Esteban-Parra MJ, Castro-Díez Y, Gámiz-Fortis SR (2022) Extreme rainfall indices in Southern Levant and related large-scale atmospheric circulation patterns: a spatial and temporal analysis. *Water* 2022(14):3799. <https://doi.org/10.3390/w14233799>
- Sasanya BF, Awodutire PO, Ufuoma OG (2024) Modelling rainfall in selected agricultural hubs in Nigeria: a comparative probability distributions study. *Theor Appl Climatol*:1–14. <https://doi.org/10.1007/s00704-024-04832-x>
- Schimmel JP (2018) Life in dry soils: effects of drought on soil microbial communities and processes. *Annu Rev Ecol Evol Syst* 49(1). <https://doi.org/10.1146/annurev-ecolsys-110617-062614>
- Schweinsberg M, Feldman M, Staub N, van den Akker OR, van Aert RC, Van Assen MA, Liu Y, Althoff T, Heer J, Kale A, Schulte-Mecklenbeck M (2021) Same data, different conclusions: radical dispersion in empirical results when independent analysts operationalize and test the same hypothesis. *Organ Behav Hum Decis Process* 165:228–249. <https://doi.org/10.1016/j.obhdp.2021.02.003>
- Sharma P, Singh AK, Agrawal B, Sharma A (2020) Correlation between weather and COVID -19 pandemic in India: An empirical investigation. *Journal of Public Affairs*. <https://doi.org/10.1002/pa.2222>
- Shen SSP, Howard A, Yin H, Khurshed F, Akbar M (2003) Statistical analysis of drought indices and Alberta drought monitoring. *Alberta Agriculture, Food and Rural Development*: Edmonton, AB, Canada, 1:7–13
- Sneha B, Uma G (2023) Analysing the impact of rainfall patterns on agriculture, economy and tourism in India: a statistical approach. *Int J Environ Clim Change* 13(11):4626–4637. <https://doi.org/10.9734/ijec/2023/v13i113642>
- Szép IJ, Mika J, Dunkel Z (2005) Palmer drought severity index as soil moisture indicator: physical interpretation, statistical behaviour and relation to global climate. *Phys Chem Earth* 30:231–243. <https://doi.org/10.1016/j.pce.2004.08.039>
- Tabari H (2020) Climate change impact on flood and extreme precipitation increases with water availability. *Sci Rep* 10:13768. <https://doi.org/10.1038/s41598-020-70816-2>
- Tam BY, Szeto K, Bonsal B, Flato G, Cannon AJ, Rong R (2019) CMIP5 drought projections in Canada based on the standardized precipitation evapotranspiration index. *Can Water Resour J* 44, 90(1):–107. <https://doi.org/10.1080/07011784.2018.1537812>
- Tao L, Ryu D, Western A, Boyd D (2021) A new drought index for soil moisture monitoring based on MPDI-NDVI trapezoid space using modis data. *Remote Sens* 13(1):122. <https://doi.org/10.3390/rs13010122>
- Tirivarombo S, Osupile D, Eliasson P (2018) Drought monitoring and analysis: standardised precipitation evapotranspiration index (SPEI) and standardised precipitation index (SPI). *Physics and Chemistry of the Earth* 106:1–10. <https://doi.org/10.1016/j.pce.2018.07.001>
- Van Loon, A. F., Gleeson, T., Clark, J., Van Dijk, A. I. J. M., Stahl, K., Hannaford, J., Di Baldassarre, G., Teuling, A. J., Tallaksen, L. M., Uijlenhoet, R., Hannah, D. M., Sheffield, J., Svoboda, M., Verbeiren, B., Wagener, T., Rangecroft, S., Wanders, N., & Van Lanen, H. A. J. (2016). Drought in the Anthropocene. In *Nature Geoscience* (Vol. 9, Issue 2). <https://doi.org/10.1038/ngeo2646>
- Vargas R, Enrique SCP, Serrano-Ortiz P, Yuste JC, Domingo F, López-Ballesteros A, Oyonarte C (2018) Hot-moments of soil CO₂ efflux in a water-limited grassland. *Soil Syst* 2(3):47. <https://doi.org/10.3390/soilsystems2030047>
- Vicente-Serrano SM, Beguería S, López-Moreno JI (2010) A multi-scalar drought index sensitive to global warming: the standardized precipitation evapotranspiration index. *J Clim* 23(7):1696–1718. <https://doi.org/10.1175/2009JCLI2909.1>
- Vicente-Serrano SM, Miralles DG, Domínguez-Castro F, Azorin-Molina C, El-Kenawy A, McVicar T, Tomás-Burguera M, Beguería S, Maneta M, PeñaGallardo M (2018) Global assessment of the standardized evapotranspiration deficit index (SEDI) for drought analysis and monitoring. *J Clim* 31(14):5371–5393. <https://doi.org/10.1175/jcli-d-17-0775.1>
- Vincent LA, Peterson TC, Barros VR, Marino MB, Rusticucci M, Carrasco G, Ramirez E, Alves LM, Ambrizzi T, Berlatto MA, Grimm AM, Marengo JA, Molion L, Moncunill DF, Rebello E, Anunciação YMT, Quintana J, Santos JL, Baez J et al (2005) Observed trends in indices of daily temperature extremes in South America 1960–2000. *J Clim* 18(23):5011–5023. <https://doi.org/10.1175/JCLI3589.1>
- Wang H, Vicente-serrano SM, Tao F, Zhang X, Wang P, Zhang C, Chen Y, Zhu D, Kenawy AE (2016) Monitoring winter wheat drought threat in Northern China using multiple climate-based drought indices and soil moisture during 2000–2013. *Agric Forest Meteorol*:228–229. <https://doi.org/10.1016/j.agrformet.2016.06.004>
- Welch B, Gauci V, Sayer EJ (2018) Tree stem bases are sources of CH₄ and N₂ O in a tropical forest on upland soil during the dry to wet season transition. *Glob Chang Biol* 25(1):361–372. <https://doi.org/10.1111/gcb.1449>
- Wu T, Zheng W, Yin W, Zhang H (2021) Spatiotemporal characteristics of drought and driving factors based on the GRACE-derived total storage deficit index: a case study in Southwest China. *Remote Sens* 2021(13):79. <https://doi.org/10.3390/rs13010079>
- Yadav R, Tripathi SK, Pranuthi G, Dubey SK (2014) Trend analysis by Mann-Kendall test for precipitation and temperature for thirteen districts of Uttarakhand. *Journal of Agrometeorol* 16(2):164–171. <https://doi.org/10.54386/jam.v16i2.1507>
- Yin H, Sun Y (2018) Characteristics of extreme temperature and precipitation in China in 2017 based on ETCCDI indices. *Adv Clim Chang Res* 9(4):218–226. <https://doi.org/10.1016/j.accr.2019.01.001>
- Yu B, Liu G, Liu Q (2018) Effects of land use changes for ecological restoration on soil moisture on the Chinese Loess Plateau: a meta-analytical approach. *J For Res* 31(2):443–452. <https://doi.org/10.1007/s11676-018-0760-0>
- Zakwan M, Ara Z (2019) Statistical analysis of rainfall in Bihar. *Sustainable Water Resources Management* 5(4):1781–1789. <https://doi.org/10.1007/s40899-019-00340-3>
- Zeri M, Alvalá RCS, Carneiro R, Cunha-Zeri G, Costa JM, Spatafora LR, Urbano D, Vall-Llossera M, Marengo J (2018) Tools for communicating agricultural drought over the Brazilian Semiarid using the soil moisture index. *Water (Switzerland)* 10(10):1421. <https://doi.org/10.3390/w10101421>
- Zhang R, Zhao C, Ma X, Brindha K, Han Q, Li C, Zhao X (2019) Projected spatiotemporal dynamics of drought under global warming in Central Asia. *Sustainability (Switzerland)* 11(16):4421. <https://doi.org/10.3390/su11164421>

Springer Nature or its licensor (e.g. a society or other partner) holds exclusive rights to this article under a publishing agreement with the author(s) or other rightsholder(s); author self-archiving of the accepted manuscript version of this article is solely governed by the terms of such publishing agreement and applicable law.